Chapter 5

Molecular Theory of Acyl Chain Packing in Lipid and Lipid-Protein Membranes

Deborah R. Fattal and Avinoam Ben-Shaul

CONTENTS

I. INTRODUCTION

In this chapter we describe a molecular level theory of lipid packing and chain statistics in membrane bilayers and demonstrate some of its recent biophysical applications.[1,2] The central quantity in this "mean field" theory is the singlet probability of lipid tail conformations. The singlet probability distribution function is derived by minimizing the system free energy subject to the relevant packing constraints on lipid conformational statistics. As will be shown in the next section, these packing constraints can be expressed in a simple mathematical form, based on one reasonable and commonly accepted physical assumption — namely, that the hydrophobic score of the lipid membrane (in its fluid state) is uniformly packed by chain segments at liquid-like density.[3-5] This assumption implies packing constraints which depend on the aggregation geometry, that is, on the curvature of the hydrocarbon-water interface and on the average area per headgroup, as measured at this interface. This yields a mathematically simple expression for the singlet probability distribution, with the aid of which one can calculate any desired conformational property and, in the mean field approximation, any thermodynamic property of interest.

Previous applications of this theory include amphiphile chain packing statistics (e.g., bond orientational order parameters and segment spatial distributions) in micelles, bilayers, and monolayers;[1,2] curvature and stretching elasticity of pure and mixed membranes;[6] and a simple model for lipid protein interaction that will be described in Section 4.[7] Recently, the theory has been extended to monolayers of grafted polymers ("brushes").[8]

Being a mean field theory, the approach described here is obviously approximate as far as thermodynamic properties are concerned. As has been and will be demonstrated (Section 3), its predictions with regard to "single chain" conformational properties, which depend only on the singlet distribution, show good agreement with both experiments and large-scale computer simulations. As a molecular level theory it is certainly more detailed than phenomenological, e.g., continuum theories of the lipid membrane or models based on geometric packing considerations.[3-5] On the other hand, it is less detailed (yet much simpler to implement) than many-molecule computer simulations, such as molecular dynamics (MD) or Monte Carlo (MC) calculations.

In MD simulations of a lipid membrane one solves the classical equations of motion governing the dynamics of all the atoms of all the constituent lipid molecules, as well as those of the surrounding water molecules (see, e.g., References 9 to 13). To avoid finite size effects the simulated membrane should include at least several hundred lipids and a similar number of water molecules. The computation times are enormous even on the fastest present-day computers,[9] and the corresponding physical times sampled are rather short (a few hundred picoseconds). Another, inevitable difficulty associated with these

0-8493-4731-9/96/$0.00+$.50

calculations are the uncertainties involved with the multitude of intermolecular potentials required for such calculations, especially those governing the interfacial (aqueous) regions of the membrane.[13] The long equilibration times and the uncertainties in interaction potentials can sometimes lead to computational artifacts but, most importantly, considerably limit the number of systems and conditions (e.g., membrane shapes) which can be faithfully modeled. Nevertheless, with the fast advent of computers and computing algorithms, MD simulations are rapidly becoming more common and more reliable and will certainly play an increasing central role in providing information on the dynamics and structure of complex many-molecule systems, including lipid and lipid-protein membranes.

The uncertainties in intermolecular potentials also affect the applicability of MC simulations. In these simulations, unlike in MD, one does not solve the equations of motions, but, rather, tries to sample as many equilibrium configurations of the system in question as possible (see, e.g., References 14 to 16). Various algorithms have been developed to efficiently "move" from one configuration to another. A major difficulty in MC studies of lipid membranes is related to the high, liquid-like density of these systems and the polymeric character of the lipid chains. These facts impose severe limitations on the MC sampling procedure, which in some cases may result in "unexplored" phase space regions. Yet, as with the MD simulations, increasingly sophisticated MC procedures are constantly being developed, and it can be anticipated that many important (especially structural) properties of lipid membranes will be investigated using these methods.

In mean field theories of the lipid membrane one treats, usually in great detail, the conformational properties of one "central" molecule, but the effects of neighboring molecules are treated approximately. They are assumed to provide a "mean field" for the "motion" of the central molecule. In general, the mean field appears as a variational parameter (or parameters) in the singlet probability distribution of the central chain and its numerical evaluation involves a solution of "self-consistency" equations. For instance, in the theory presented in the next section, the mean field acting on the central lipid molecule is represented by the "lateral pressure profile" exerted on this chain by its neighbors. (As the average area per molecule decreases, the lateral pressure increases, and the lipid chains are stretched further along the membrane normal.) The self-consistency equations represent the packing constraints on the lipid chains which, as mentioned above, reflect the assumption of a uniform, liquid-like, hydrophobic core.

Several mean field theories of chain packing statistics in bilayers have been formulated to account for structural and thermodynamic properties of lipid membranes. The first theory of this kind was proposed by Marelja,[17,18] primarily in order to analyze the fluid-solid ("gel-liquid crystalline") transition in lipid bilayers. This theory, formulated in the spirit of the Maier-Saupe theory of the isotropic to nematic phase transition in liquid crystals,[19] assumes that interchain interactions are governed by the anisotropy of the interaction potential between neighboring chain segments. In this respect it is different from the theory described below in which excluded volume (packing) interactions are the dominant ones. These interactions also play the decisive role in the lattice theory originally presented by Dill and Flory[20] and then further developed by Dill and Stigter.[21] Gruen's theory,[22,23] developed at about the same time, is in many respects similar to ours,[24-32] as has been discussed in detail elsewhere.[30] Another mean field approach, extensively applied to analyze lipid membrane properties, has been developed by the Wageningen group, based on the mean field theory of polymeric systems originally proposed by the Scheutjens and the Fleer (see, e.g.,References 33 to 36). Unlike our approach, this theory is based on the assumption that the lipid chain segments occupy the sites of a given underlying lattice.

Most of the mean field theories mentioned above share several common features and differ in some other (often subtle) respects. Our intention in this chapter is not to compare the different theories but, rather, to describe one consistent approach, its possible applications, and some of its achievements as well as possible deficiencies. To this end, after introducing the basic theoretical concepts in Section 2, we will describe three different applications of biological relevance in Sections 3 to 5 and conclude with some preliminary results relevant to the application of the theory to vesicle fusion in Section 6.

II. MOLECULAR THEORY OF MEMBRANE STRUCTURE

In this section we describe a rather simple statistical thermodynamic molecular theory of lipid chain packing in membranes in their fluid state. As usual, we treat the membrane as a two-dimensional (2D) film, composed of a central hydrophobic region comprising the hydrocarbon chains ("tails") of the lipid molecules and two interfacial regions containing the lipid polar headgroups (Figure 1). We shall focus on the conformational properties of the lipid chains. The interactions involving the polar heads will only

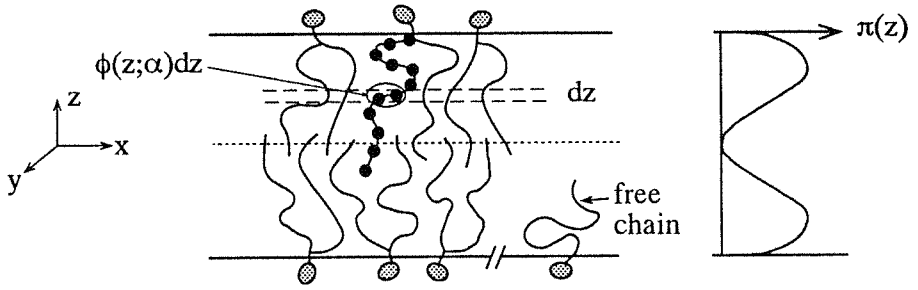

Figure 1 Schematic illustration of a (planar) lipid bilayer and the quantities appearing in the derivation of the singlet probability of chain conformations (see Equation 5): $\phi(z;\alpha)dz$ denotes the number of chain segments which, for a chain in conformation α, fall within the shell $z,z + dz$. The 'free chain' is a (hypothetical) chain with no neighbors around it. The lateral pressure profile $\pi(z)$ schematically illustrated in the figure accounts for the pressure exerted on a given (stretched) chain by its neighbors in the bilayer.

be treated in an approximate, "phenomenological" fashion. The main reason for that is the highly specific nature of these interactions which depend sensitively on the size, charge (e.g., ionic vs. zwitterionic), and chemical composition of the headgroups. On the other hand, the theoretical treatment of the hydrophobic region of the membrane is in many respects simpler and more general. This is because the hydrophobic core is, to a very good approximation, uniformly packed with lipid chain segments at hydrocarbon liquid-like density.[3-5] This basic fact is valid and thus simplifies considerably the theoretical description, even when the core is composed of different types of acyl chains (e.g., saturated and partially unsaturated or long and short chains).

The membrane free energy can be expressed as a sum of three terms,

$$F = F_t + F_s + F_h = 2N\left(f_t + f_s + f_h\right) \tag{1}$$

representing, respectively, the contributions of the hydrocarbon tails, the surface free energy corresponding to the hydrocarbon-water interface, and the (solution-mediated) interaction free energy between the headgroups. f_i (= t,s,h) denotes the corresponding free energies, per molecule, with $2N$ denoting the number of molecules in the membrane (N per monolayer, on average). All three terms depend on the lipid composition of the two monolayers comprising the membrane bilayer and the ambient solution conditions, as well as on the membrane area and curvature. The interplay between these terms dictates the equilibrium geometry of the membrane (area and curvature), fluctuations around the equilibrium state, and all microscopic (e.g., chain conformations) and thermodynamic (e.g., elastic) properties of the membrane. We shall first consider each term separately, devoting most of the discussion to F_t.

B. CHAIN FREE ENERGY

The formalism outlined below can be applied to a bilayer membrane of arbitrary lipid composition, whether symmetric or nonsymmetric with respect to the two monolayers, as well as to an arbitrary membrane thickness and/or curvature. Also, the theory can be and has been applied to other amphiphilic aggregates such as micelles (see also Section V), as well as to systems containing hydrophobic solutes (see Section IV). Yet, to introduce the basic concepts involved and to derive the main working equations and expressions, let us consider the simplest possible membrane: namely, a planar and symmetric bilayer composed of a single lipid component. To further simplify the description, let us assume that the lipids are single (saturated) chain amphiphiles of the form $\mathcal{P}$–$(CH_2)_{n-1}$–CH_3, with $\mathcal{P}$ symbolizing the polar headgroup. The generalization to doubly tailed lipids, including nonsaturated lipid chains, is straightforward, as described in Section III.

Our goal is to derive an expression for $P(\alpha)$, the probability of finding the lipid hydrocarbon chain in conformation α. In general, $P(\alpha)$ is fully specified by the coordinates of all the atoms constituting the tail. In practice, one can employ rather accurate but simpler schemes like the rotational isomeric state (RIS) model of acyl chains,[37] whereby α is specified by the trans/gauche sequence of the CH_2–CH_2 bonds along the chain and by the overall orientation of the chain (specified by three Euler angles) relative to some arbitrary fixed system of coordinates (see Figure 1). For a lipid of the form $\mathcal{P}$–$(CH_2)_{n-1}$–CH_3 the number of trans/gauche sequences is 3^{n-1} (treating the P–$(CH_2)_1$ bond as a CH_2–CH_2 bond). In the numerical

examples presented in the following sections, the calculations involve generation of all possible sequences, each multiplied by several dozens overall chain orientations as well as several lateral displacements of the headgroup relative to the hydrocarbon-water interface.[31]

Knowing the equilibrium $P(\alpha)$ we can calculate any desirable "single-chain" conformational property. Of particular interest are those properties which can be either measured experimentally or calculated by detailed computer simulations. In addition to the physical significance of these properties, their calculation provides a test for the expression which we will soon derive for $P(\alpha)$. The most commonly measured or calculated conformational properties are the bond orientational order parameters and the segment spatial distributions to be defined later. Furthermore, $P(\alpha)$ can be used to calculate various thermodynamic properties of interest, such as the free energy per chain, f_t, and related quantities such as the curvature elasticity moduli of the membrane.[6,38-41]

The free energy per chain is given, in terms of $P(\alpha)$, as

$$f_t = \sum_{\alpha} P(\alpha)\epsilon(\alpha) + kT\sum_{\alpha} P(\alpha)\ln P(\alpha) \tag{2}$$

where k is Boltzmann's constant, T is the temperature, and $\epsilon(\alpha)$ is the internal (trans/gauche) energy of a chain in conformation α. More specifically, $\epsilon(\alpha) = n_g(\alpha)e_g + n_t(\alpha)e_t$, where $n_g(\alpha)$ and $n_t(\alpha)$ are the numbers of gauche and trans conformers along the chain, with e_g and e_t representing their respective energies. One usually sets $e_t = 0$, implying that $e_g \simeq 500$ cal/mol.

The first term in Equation 2 is the energetic contribution to the chain free energy, while the second is the conformational entropy contribution. Both depend on the curvature of the membrane, its thickness, and its chemical composition.

Equation 2 representing the chain free energy as a function of the singlet probability distribution (spd) of chain conformations, is also the key expression in the variational procedure for deriving the equilibrium expression for $P(\alpha)$. We derive the desired (equilibrium) spd by minimization of f_t with respect to $\{P(\alpha)\}$, subject to whichever constraints $P(\alpha)$ must fulfill. Except for the trivial normalization condition ($\sum_\alpha P(\alpha) = 1$) the only additional constraint which we impose on $P(\alpha)$ results from one simple and common assumption. Namely, we assume that the liquid-like hydrophobic core is uniformly packed by chain segments. The mathematical expression of this constraint is

$$\int ds\sigma(\mathbf{s})\sum_{\alpha} P(\alpha;\mathbf{s})\psi(\mathbf{r};\alpha,\mathbf{s}) = \rho(\mathbf{r}) \quad (\text{all } \mathbf{r}) \tag{3}$$

which for a symmetric planar bilayer reduces to

$$\sum_{\alpha} P(\alpha)\left[\phi(z;\alpha) + \phi(-z;\alpha)\right] = a\rho \quad (\text{all } z) \tag{4}$$

The quantities appear in Equations 3 and 4 are as follows: $P(\alpha;\mathbf{s})$ denotes the spd corresponding to chains originating from point $\mathbf{s}$ of the hydrocarbon-water interface; for simplicity $\mathbf{s}$ may be regarded as the headgroup position. $\sigma(\mathbf{s})$ is the lateral density of headgroups at the interface; i.e., $\sigma(\mathbf{s})ds$ is the number of chains originating from an area element ds at the interface. It should be noted that the $\mathbf{s}$ integration in Equation 3 includes both interfaces. The quantity $\psi(\mathbf{r};\alpha,\mathbf{s})d\mathbf{r}$ denotes the number of segments of a chain in conformation α, originating at $\mathbf{s}$, which fall within a small volume element $d\mathbf{r}$ (around $\mathbf{r}$) of the hydrophobic core. $\rho(\mathbf{r})$ is the average segment density at $\mathbf{r}$ which, for a "compact" core, is constant: $\rho(\mathbf{r}) = \rho = 1/v$, where v is the average volume per chain segment in the hydrophobic core.

In passing from Equation 3 to Equation 4 we have specifically considered a symmetric planar single-component bilayer. For this system we have $\sigma(\mathbf{s}) = constant = 1/a$, where a is the average cross-sectional area per chain, measured at the hydrocarbon-water interface. This important structural characteristic of the membrane is usually referred to as "the area per headgroup." Also, for the simple bilayer, $P(\alpha;\mathbf{s}) = P(\alpha)$ is independent of $\mathbf{s}$. We now choose a coordinate system whose origin is at the bilayer midplane, with its z axis pointing towards the "upper" interface. Clearly, for a chain with headgroup coordinates $6\mathbf{s} = x,y = 0,0$ the quantity $\psi(\mathbf{r},\alpha\mathbf{s}) = \psi(\mathbf{r},\alpha,0)$ is only a function of z. Then the left-hand side of Equation

3 can be integrated over x and y to obtain Equation 4, in which $\phi(z;\alpha)dz = [\int \psi(\mathbf{r};\alpha)dxdy]dz$ is simply the number of segments of an α-chain falling within the shell $z,z + dz$ of the hydrophobic core (see Figure 1). The two terms within the square brackets in Equation 4 represent the contribution to the segment density in z due to chains anchored to the "upper" and "lower" interfaces, respectively. Of course Equation 4 could be immediately written down for the symmetric bilayer. We have emphasized here that it is a special case of the more general form Equation 3, which will be of use in Section IV.

To derive $P(\alpha)$ we now minimize Equation 2 subject to Equation 4 and obtain

$$P(\alpha) = \frac{1}{q}\exp\left[-\beta\epsilon(\alpha) - \beta\int \pi(z)\phi(z;\alpha)dz\right] \tag{5}$$

with

$$q = \sum_{\alpha}\exp\left[-\beta\epsilon(\alpha) - \beta\int \pi(z)\phi(z;\alpha)dz\right] \tag{6}$$

representing the conformational partition function of the chain, and $\beta \equiv 1/kT$. The quantities $\{\pi(z)\}$ in these equations are the Lagrange multipliers conjugated to the packing constraints Equation 4. They have the dimensions and the physical significance of "lateral pressures", as discussed in detail elsewhere[1,2,24,25] (see Figure 1).

The numerical values of the $\{\pi(z)\}$ terms are determined by the self-consistency equations resulting from substitution of Equation 5 into the packing constraint (Equation 4). This results in a set of nonlinear algebraic equations which can be solved quite simply and efficiently for any chain model.

Substituting Equation 5 into Equation 2 we obtain

$$f_I = -kT\ln q - a\rho\int \pi(z)\,dz \tag{7}$$

Thus, after evaluating the $\pi(z)$ we can calculate any chain conformational property derivable from $P(\alpha)$ through Equation 5 or any thermodynamic property derivable from f_I using Equation 7. Clearly, all the results depend sensitively, through $\pi(z)$, on the value of the area per headgroup, a.

The results of Equations 5 to 7, corresponding to the symmetric, planar, single-component bilayer, can be easily generalized to more complex systems. Let us briefly mention a few cases of interest.

Curved bilayers — In this case, instead of a constant cross-sectional area per chain, a, we have $a = a(c_1,c_2,z)$, where c_1 and c_2 denote the local interfacial curvatures $c_i = 1/R_i$ are the principal curvatures; R_i denotes the radius of curvature). In this case the packing constraints (Equation 4) should be replaced by

$$\chi_E\sum_{\alpha}P_E(\alpha)\phi(z;\alpha) + \chi_I\sum_{\beta}P_I(\beta)\phi(z;\beta) = \rho a(z) = a(0)\left[1 + (c_1 + c_2)z + c_1c_2z^2\right] \tag{8}$$

with $P_E(\alpha)$ and $P_I(\beta)$ representing the spd's of chains originating at the "external" (E) and "internal" (I) monolayers comprising the bilayer, e.g., of a vesicle. (Clearly, for a spherical vesicle of radius R,$c_1 = c_2 = 1/R$.) The quantities χ_E and χ_I are the "mole fractions" of lipids in the two monolayers; $\chi_e = N_E/N$ and $\chi_I = N_I/N$ ($\chi_E + \chi_I = 1$, $N_E + N_I = N$), with N_E and N_I denoting the number of chains originating from the E and I interfaces, respectively.

The free energy of the system in this case is given by

$$F_I = N_E\sum_{\alpha}P_E(\alpha)\left[\epsilon(\alpha) + kT\ln P_E(\alpha)\right] + N_I\sum_{\beta}P_I(\beta)\left[\epsilon(\beta) + kT\ln P_I(\beta)\right] \tag{9}$$

Minimization of Equation 9 with respect to Equation 8 yields for $P_E(\alpha) = P_E(\alpha;a,c_1,c_2)$ and $P_I(\beta) = P_I(\beta;a,c_1,c_2)$ expressions similar to Equation 5, except that now $\pi(z)$ and $q_E(q_I)$ depend not only on a but also on c_1 and c_2.

Micelles — Here again, all we need to do is to account for the curvature dependence of $a(z)$. For a cylindrical micelle, for instance, as will be discussed in Section V, instead of Equation 4 we have

$$\sum_{\alpha} P(\alpha)\phi(\pi;\alpha) = \rho a(R) r / R \tag{10}$$

where R is the radius of the micelle and r is the radial distance from the cylinder axis. Here again $P(\alpha)$ has the same form as Equation 5, but now the pressure profile $\{\pi(r)\}$ depends on the micellar radius R. For micelles composed of chains of a given length n the average area per chain at the interface, $a(R)$, is uniquely determined by R through the geometric packing condition $a(R) = 2v/R$, where v is the chain volume. For simple alkyl chains, $-(CH_2)_{n-1}-CH_3$, $v \cong (n + 1)v$, where $v \simeq 27$ Å^3 is the specific volume of a CH_2 group.

Two- (or more) component systems — Consider for instance a planar symmetric bilayer composed of two types of lipid chains, A and B. Then, instead of Equation 4 we write

$$X_A \sum_{\alpha} P_A(\alpha)\left[\phi_A(z,\alpha) + \phi_A(-z;\alpha)\right] + X_B \sum_{\beta} P_B(\beta)\left[\phi_B(z,\beta) + \phi_B(-z,\beta)\right] = a\rho \tag{11}$$

where X_A and $X_B = 1 - X_A$ denotes the mole fractions of the two types of chains. The free energy of this system is given by

$$F_t = N\left(X_A f_{t,A} + X_B f_{t,B}\right) \tag{12}$$

with $f_{t,A}$ and $f_{t,B}$ defined according to Equation 2. Again, minimization of Equation 12 subject to Equation 11 yields $P_A(\alpha)$ and $P_B(\beta)$ of the Equation 5 form. The same $\pi(z)$ appears in both expressions.

Nonuniform membranes — The presence of a hydrophobic solute in the membrane — say, an integral protein, — "breaks" the translational symmetry of the planar bilayer. Thus, $P(\alpha,\mathbf{s})$ will depend on the headgroup position $\mathbf{s}$, as measured, for instance, with respect to the position of the protein. In this more general case, we have

$$F_t = \int d\mathbf{s}\sigma(\mathbf{s}) f_t(\mathbf{s}) \tag{13}$$

where $f_t(\mathbf{s})$ is the local free energy of a chain originating at $\mathbf{s}$. The relevant packing constraint is now Equation 3. Minimization of Equation 13 with respect to Equation 3 yields[7]

$$P(\alpha;\mathbf{s}) = \frac{1}{q(\mathbf{s})} \exp\left[-\beta\epsilon(\alpha) - \beta \int d\mathbf{r}\lambda(\mathbf{r})\psi(\mathbf{r};\alpha,\mathbf{s})\right] \tag{14}$$

with the $\lambda(\mathbf{r})$ corresponding to the Lagrange parameters conjugated to the packing constraints (Equation 3). In this case, due to the lower symmetry of the system, the calculations are considerably more involved (chains must be generated and classified for different points $\mathbf{s}$), but are feasible, as illustrated in Section 4 for a model of lipid protein interaction.[7]

B. ADDING F_s AND F_h

The conformational free energy f_t, as given by Equations 2 and 7, decreases as the average cross-sectional area per chain, a, increases. This follows simply from the fact that as a increases the lateral dimensions of the chains also increase, allowing for more conformational freedom. More precisely, the energetic contribution to the free energy $\langle\epsilon_t\rangle = \sum P(\alpha)\epsilon(\alpha)$ increases with a since the average number of gauche bonds increases. However, the increase in conformational entropy (chain flexibility) overcompensates for the increase in $\langle\epsilon_t\rangle$, resulting in a net decrease of f_t. Thus, the conformational free energy corresponds effectively to a repulsive interaction between chains. This implies a positive lateral pressure

$$\Pi_t = -\frac{\partial f_t}{\partial a} = -\rho \int \pi(z) dz > 0 \tag{15}$$

which tends to expand the bilayer.

The interaction between the headgroups, whether electrostatic or steric, is generally also repulsive;[1-3] i.e.,

$$\Pi_h = -\frac{\partial f_h}{\partial a} > 0 \tag{16}$$

where $f_h = F_h/2N$ is the average interaction free energy per headgroup.

The interfacial free energy F_s provides the force which opposes both interheadgroup and interchain repulsions. The origin of this force is the "hydrophobic interaction", resulting from the increased hydrocarbon-water contact area upon increasing a. $f_s = F_s/2N$ is usually expressed as a simple surface energy $f_s = \gamma a$, with γ (often taken as $\gamma = 50$ dyn/cm = 0.12 kT/Å^2 at T = 300 K) denoting the effective surface tension.[3] With this representation of f_s one has

$$\Pi_s = -\frac{\partial f_s}{\partial a} = -\gamma < 0 \tag{17}$$

The equilibrium area per headgroup, a_{eq}, is determined by the balance of the three forces, that is,

$$\Pi_t + \Pi_h + \Pi_s = 0 \tag{18}$$

Figure 2 shows the three contributions, f_t, f_s, and f_h, to the average free energy per molecule

$$f = f_t + f_s + f_h \tag{19}$$

as a function of the area per molecule in a planar bilayer. The chain contribution $f_t(a)$ was calculated using Equation 6 for three values of chain length (n = 12,14,16). The hydrocarbon tails correspond to simple alkyl chains, $-(CH_2)_{n-1}-CH_3$, modeled using the rotational isomeric state model. For f_s we have used $f_s = \gamma a$ with $\gamma = 0.12$ kT/Å^2. The headgroup contribution is represented here by the simple (and common) form[3,5,7]

$$f_h = C/a \tag{20}$$

where C is a phenomenological constant. For the calculations shown in Figure 2 it has been chosen to yield a_{eq} = 32 Å^2 for the n = 14 chains (C = 48 kT).

It should be stressed that Equation 20 is a highly approximate representation of f_h. Several authors have suggested more elaborate expressions for f_h, based on detained models for electrostatic and/or steric repulsions (see, e.g., References 31 and 42 to 49). Unfortunately, these expressions are usually system specific and contain some poorly known molecular parameters. Thus, in some respects it is more reasonable to Equation 20 (or alternative phenomenological expressions; see Section 5) and treat C as a semiempirical parameter, as we did in Figure 2.

A rather common approximation in phenomenological treatments of amphiphile self-assembly is to set f_t to be a constant, independent of chain length and structure as well as of aggregation geometry. Thus, in bilayers, for example, f_t is assumed to be independent of chain length and of the area per headgroup a. In this case, using Equation 19 for f for Equation 20 for f_h, and setting $f_s = \gamma a$, one finds that $a_{eq} = (C/\gamma)^{1/2}$, independent of chain length. Experiments suggest that in lipid bilayers a_{eq} is indeed nearly independent of chain length.[3,50] In the calculations shown in Figure 2 the chain term, f_t, is explicitly included and as can be seen $f_t(a)$ depends sensitively on a. Yet the value of a_{eq} varies only weakly with n. In fact, based on simple scaling arguments it can be shown that $a_{eq} \sim n^{\alpha}$ with $\alpha \leq 1/3$, explaining the very slow increase of a_{eq} with n.[2,31] Furthermore, our calculations suggest that chain repulsion is actually stronger than headgroup repulsion, i.e., $\Pi_t > \Pi_h$. Thus, the slow variation of a_{eq} with n should not be regarded as justification for the approximation f_t = *constant*. As noted above, in this approximation, also known as

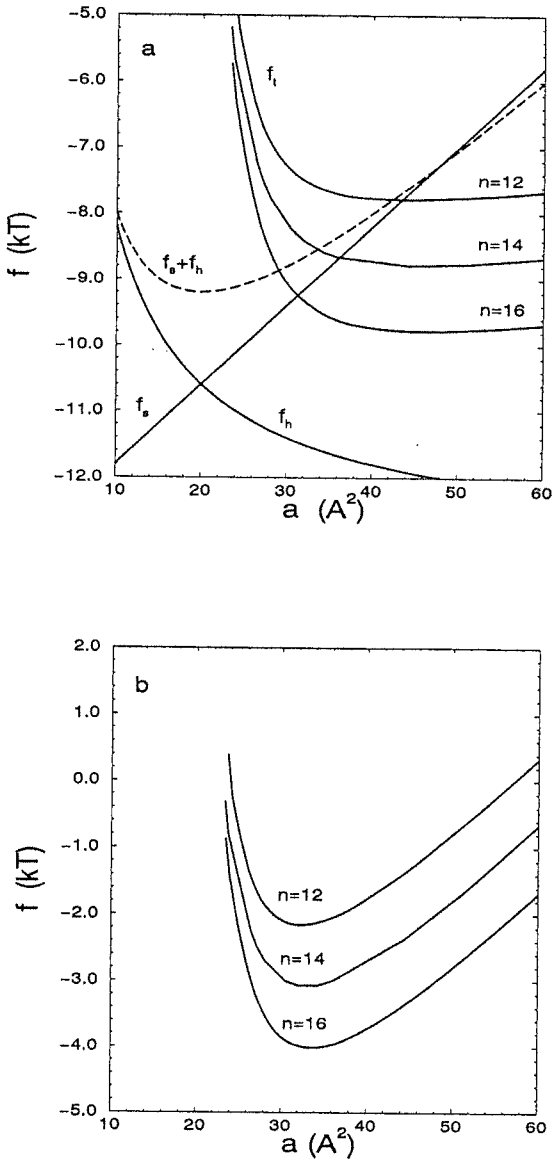

Figure 2 (a) The variation of the chain (f_t), headgroup (f_h) and surface (f_s) contributions to the average free energy per molecule, as a function of the average cross sectional area per chain (headgroup), a (see Equation 19). f_h is calculated using Equation 20 with $C = 48$ kT. $f_s = \gamma a$ with $\gamma = 0.12$ kT/Å^2. f_t is calculated using the meanfield theory for C_{12}, C_{14}, and C_{16} chains. (b) The sum of the three contributions above revealing that a_{eq} (~32 Å^2) increases slowly with chain length. (From Ben-Shaul, A., *Handbook of Physics of Biological Systems,* Vol. 1, Lipowsky, R. and Sackman, E., Eds., Elsevier Science, Amsterdam, 1995, Chap. 7. With permission.)

"the hydrocarbon droplet assumption",[3-5] the chain conformational properties are assumed to be independent of the hydrophobic core geometry. Considering the fact that the dimensions of the hydrophobic region are comparable to the hydrocarbon chain length, there is no *a priori* justification for this assumption.

From the variation $\delta f(a) = f(a) - f(a_{eq})$ of $f(a)$ around the equilibrium area, $a = a_{eq}$, one can evaluate the area compressibility modulus κ_a defined by[38]

$$\frac{1}{a_{eq}}\delta f(a) = \frac{1}{2}\kappa_a\left(\frac{\delta a}{a_{eq}}\right)^2 \tag{21}$$

From the data in Figure 2 it follows that $\kappa_a \sim 0.2$ kT/Å^2. One can also calculate $\delta f(a,c_1,c_2) = f(a,c_1,c_2) - f(a_{eq},c_1^{eq},c_2^{eq})$ and thus derive explicit expressions and numerical values for curvature elasticity moduli. The relevant formalism and its applications have been described in detail elsewhere.[2,6] The calculation of membrane elastic moduli is a particular *thermodynamic* application of the theory outlined in this section. Other thermodynamic applications are described in Sections 4 and 5. Clearly, these calculations are only approximate, since the free energy is calculated using the *singlet* probability distribution function $P(\alpha)$ rather than the multichain distribution $P(\alpha_1,\ldots,\alpha_N)$. It should be stressed that these "mean field" calculations of the free energies and related thermodynamic functions are approximate even if $P(\alpha)$ were the exact singlet distribution

$$P(\alpha) = \sum_{\alpha_2,\ldots,\alpha_N} P(\alpha_1 = \alpha,\alpha_2,\alpha_3,\ldots,\alpha_N) \tag{22}$$

The variational derivation of the singlet probability distribution (Equation 5) started indeed with the mean field free energy expression (Equation 2). However, an alternative derivation of Equation 5 is possible, based on expansion of the many chain configurational partition functions, lending further theoretical support to the accuracy of this form for the singlet probability distribution.[25]

In the next section we briefly describe the application of $P(\alpha)$ for calculating single-chain conformational properties and compare the results obtained to experimental and computer simulation data.

III. CHAIN CONFORMATIONAL PROPERTIES

One of the most familiar characteristics of conformational chain statistics in membranes is the bond orientational order profile of the C–H bonds along the lipid hydrocarbon tails.[5,51-55] The orientational order parameters are commonly measured by nuclear magnetic resonance (NMR) methods, using selective (or nonselective) deuteration of the chains. Specifically, the measured quantity is the orientational order parameter of the C_k–H (C_k–D) bond for $-(CH_2)_{n-1}-CH_3$ chains, $k = 1,\ldots,n$), defined as

$$S_k = \left\langle P_2(\cos\theta_k) \right\rangle = \sum_{\alpha} P(\alpha)\left[3\cos^2\theta_k(\alpha) - 1\right]/2 \tag{23}$$

where $P_2(x) = (3x^2 - 1)/2$ is the second Legendre polynomial and $\theta_k(\alpha)$ denotes, for a chain conformation α, the angle between the kth bond and the membrane normal (the "director"). The C–H order parameters can be related to the skeletal order parameters, $\tilde{S}_k$, corresponding to the vectors $\mathbf{r}_{k-1,k+1}$ connecting carbons $k-1$ and $k+1$ of the chain: $\tilde{S}_k = -2S_k$ for all k except for the terminal methyl group ($-CH_3$), for which $\tilde{S}_n = -3S_n$.[55]

The orientational order parameter profiles provide a measure of chain flexibility, reflecting the "fluidity" of the hydrophobic core. In the perfectly ordered state of the membrane, when all lipid chains are in their all-*trans* conformation, with the chain axis along the membrane normal, one has $S_k = -0.5(\theta_k = \pi/2)$ or $\tilde{S}_k = 1$, for $k = 1,\ldots,n-1$. In the opposite limit, where bond orientations are random, $S_k = \tilde{S}_k = 0$.

Typically, bond order parameter profiles of (saturated) lipid chains in planar bilayers are characterized by a roughly constant value of S_k for about the first half of the chain (the "plateau region"), followed by a monotonic decrease of S_k towards the chain terminus. The last chain segments, those which reach and possibly cross ("interdigitate" through) the bilayer midplane, are characterized by $S_k \sim 0$, indicating nearly random bond orientations. This behavior also indicates "high fluidity" in the central part of the hydrophobic core, as compared to the regions bordering the interface, where chain orientational ordering is relatively large. The magnitude of S_k in the plateau region increases as the membrane thickness d increases or, equivalently, as the average cross-sectional area per chain, a, decreases. This behavior is to be expected, since as d increases, the hydrocarbon chains must be further stretched out, resulting in a higher degree of chain ordering along the membrane normal. Note that this trend is a direct consequence of the tight (fluid-like) packing condition of the chains within the hydrophobic core. In other words, the packing constraints rather than, say, the relative trans/gauche energy of the chains are the important determinant of chain ordering in membranes. These qualitative trends have been quantitatively analyzed and confirmed by molecular level calculations based on Equation 5.[28]

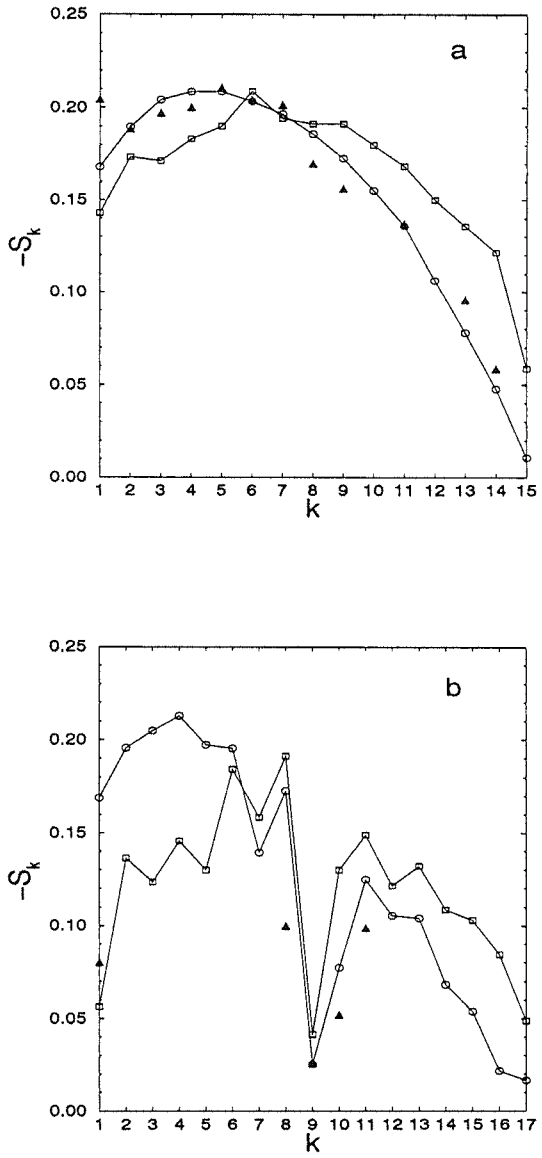

Figure 3 Orientational order parameter profiles of the C–H bonds along the palmitoyl (a) and oleoyl (b) chains of DMPC (adapted from Reference 31). ▲ — experimental results,[51] □ — molecular dynamics calculations,[9] ○ — meanfield theory. (From Fattal, D. R. and Ben-Shaul, A., *Biophys. J.*, 67, 983, 1994. With permission.)

Orientational bond order profiles calculated using Equation 5 for $P(\alpha)$ have been calculated for various sytems, including "pure" (i.e., single-component) and mixed micelles and membranes. For single-chain amphiphiles the results have been compared, whenever possible, to experimental data and computer simulation results, showing generally very good agreement.[1,2] Similarly, good agreement has been obtained with respect to other conformational properties such as segment spatial distributions and conformational energy or entropy per chain. In Figure 3 we show two sets of bond order parameter profiles, corresponding to the two hydrocarbon chains of palmitoyl-oleoyl-phosphatidylcholine (POPC).[31] Here the palmitoyl chain is a saturated $-(CH_2)_{14}-CH_3$ alkyl chain whereas the C_{17}(17-carbon) oleoyl chain contains one *cis* double bond, between carbons 8 and 9: $-(CH_2)_7-(CH{=}CH)-(CH_2)_7-CH_3$. The two chains are connected through the glycerol backbone, which is also connected to the switterionic phosphatidylcholine headgroup. The results shown in Figure 3 correspond to POPC molecules packed in a bilayer of (hydrophobic core) thickness $d = 30.0$ Å at T = 300 K. Simple packing considerations (see below) imply

that this thickness corresponds to an average cross-sectional area per headgroup of $a = 60.5$ Å^2, which is also the average cross-sectional area of the lipid tail (composed of one oleoyl and one palmitoyl chain).

The POPC bilayer has been chosen primarily in order to compare the predictions of the mean field theory (Equation 5) with those of a most comprehensive molecular dynamics (MD) simulation of the same system.[9] The MD results as well as (partial) experimental results for the POPC bilayer[51] are also shown in Figure 3. The agreement between these sets of results is quite satisfactory considering the complexity of the system modeled. The typical "plateau" region of the saturated chain is reproduced, as well as the very distinctive drop in the orientational order parameter at the double bond region of the oleoyl chain. Differences in the S_k values appear mainly for the first few C–H bonds of the oleoyl chain. This is probably due to the approximate mean field treatment of the glycerol backbone of the lipid from which the two chains emanate. In fact, in the mean field calculation of the POPC bilayer the hydrophobic core of the membrane has been modeled as an equimolar mixture of palmitoyl and oleoyl chains satisfying a packing constraint of the form in Equation 11. In other words, the connectivity of the oleoyl and palmitoyl chains through the glycerol backbone has not been explicitly taken into account. This approximation is consistent with the assumption that the interactions between chains originating from the same headgroup are no different from those originating from different headgroups. The reason for this approximation is "technical". As noted in the previous section, the calculation of $P(\alpha)$ involves the generation of all possible conformations of the chain considered. Thus, for a pure aggregate composed, say, of saturated $-(CH_2)_n-CH_3$ chains, the number of possible (RIS) conformations is of the order of 3^n. For each conformation generated one counts and classifies the $\phi(z;\alpha)$ terms into groups of degenerate conformations corresponding to their distribution within the hydrophobic core. For a mixture of $-(CH_2)_n-CH_3$ and $-(CH_2)_m-CH_3$ chains this is done separately for each type of chain. The number of conformations enumerated is thus $3^n + 3^m$. On the other hand, the total number of conformations corresponding to two chains originating from the same headgroup is $3^n \cdot 3^m$. This, of course, implies an enormous numerical effort. Furthermore, there is no real reason for treating the correlations between two chains belonging to the same headgroup more accurately than those originating from different headgroups. After all, the chains comprising the hydrophobic region are tightly packed and correlated. The mean field theory treats these correlations only indirectly, through the packing constraints, Equations 4 or 11.

We note that despite the inherent approximations involved in the mean field analysis its predictions compare well with those derived from MD simulations. The difference in computation time between the two approaches is enormous. Obviously, MD simulations provide much more detailed information, including information on dynamic properties, which the mean field equilibrium theory cannot treat at all. Yet, even with the best interaction potentials known and the fastest computers available, the number of systems which can be studied in detail by MD methods to date is limited, and even those are followed over relatively short periods of time. On the other hand, the mean field approach described above, though approximate, can be easily applied to a very wide range of systems (e.g., different lipid compositions) and a wide range of conditions (e.g., membranes of different curvatures). Thus, as noted already in Section I, while the quality of large-scale computer simulations is rapidly growing, there are many systems and properties (e.g., curvature elastic moduli) which can only be studied by approximate mean-field theories.

Another measurable structural characteristic of lipid membranes is the distribution of different chain segments across the bilayer hydrophobic core. Figure 4 shows the distribution (number of segments per unit length) of terminal (CH_3) groups, double-bonded carbons (–CH=), and the sum of all methylene (–CH_2–) segments comprising the two hydrophobic tails of dioleoyl phosphatidylcholine (DMPC). The lipid tail of these molecules is composed of two $-(CH_2)_7-(CH\triangleq CH)-(CH_2)_7-CH_3$ chains. One set of curves represents experimental results obtained by X-ray and neutron scattering.[56,57] The other represents the predictions of the mean field theory.[31] The thickness of the hydrophobic region, defined as the average distance between the lipid carbonyl groups on opposite interfaces of the membrane, is $d = 32$ Å. The agreement between the measured and calculated results is quite satisfactory, at least with respect to the peaks of the various segment distributions. The main difference appears in the width of the CH_2 distribution, showing wider "wings" of the experimental results. Yet it should be noted that no attempts were made to fit the calculated results to experiments. The only input into the calculation was the thickness of the membrane, allowing, as in other calculations of this kind, for small fluctuations of the lipid headgroup around the hydrocarbon-water interface. Further details of this and other calculations are discussed in Reference 31.

The only input parameter in the mean field calculations is the hydrophobic thickness of the membrane, d. It enters into the packing constraints (see, e.g., Equation 4) through the average cross-sectional area

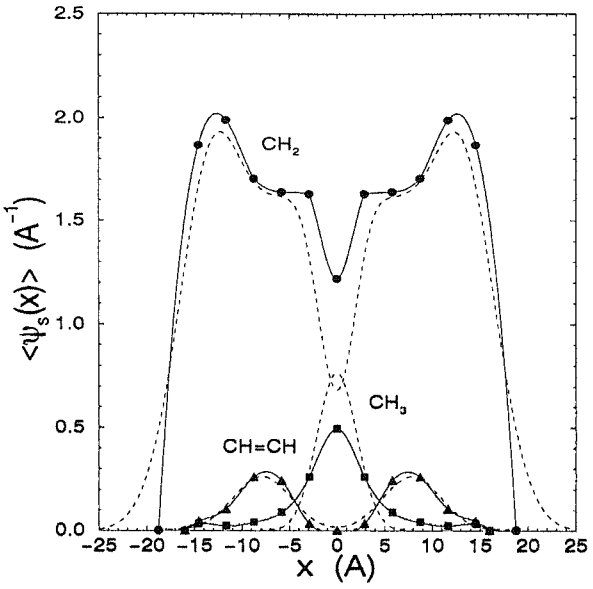

Figure 4 The distribution of lipid chain segments across a POPC bilayer (adapted from Reference 31). •, ■, and ▲ represent the results calculated by the mean-field theory for, the (sum of all) CH_2 segments, CH_3 groups, and CH=CH groups, respectively. The dashed lines are the experimental results.[57] (From Fattal, D. R. and Ben-Shaul, A., *Biophys. J.*, 67, 983, 1994. With permission.)

per chain, a. The relationship between d and a follows immediately from the assumption that the hydrophobic core is uniform and liquid like. Namely, using v to denote the volume occupied by the hydrocarbon tail, it follows immediately that $a = 2v/d$. The tail volume can be calculated by adding the specific volumes of the various segments comprising the chain, as measured for bulk liquid hydrocarbons, e.g., $v(CH_2) \cong 27$ Å^3, $v(CH_3) \cong 54$ Å^3, and $v(-CH=) \cong 21.5$ Å^3 (Reference 31, see also Reference 58). It should be noted, however, that these values are only used to convert from d to a. The quantity which actually enters the calculation is the hydrophobic thickness, d, rather than the area a. Only the relative values (not the absolute ones), e.g., $v(CH_3)/v(CH_2)$, are important for implementing the packing constraints. For further details see, e.g., Reference 31.

We conclude this section with another comparison between experimental results and mean field theory calculations. Figure 5 shows the lateral (in-plane) fluctuations of the CH_2 segments of DPPC (dipalmitoyl phosphatidylcholine) tails, packed in a planar bilayer with four different areas per chain, ranging from α = 25.5 to 31.3 Å^2 (the corresponding areas per headgroup are twice these values). More explicitly, the figure shows σ_{xy}, the root-mean-square (rms) deviations, in the xy plane (parallel to the membrane), of carbons k = 1 to 15 along the palmitoyl chain $-(CH_2)_{14}-CH_3$. The rms deviation of carbon k is calculated using

$$\left(\sigma_{xy}^{k}\right)^2 = \sum_{\alpha} P(\alpha)\left\{\left[x_k(\alpha) - \langle x_k\rangle\right]^2 + \left[y_k(\alpha) - \langle y_k\rangle\right]^2\right\} = \langle x_k^2\rangle + \langle y_k^2\rangle \tag{24}$$

with $x_k(\alpha)$ denoting the x coordinate of the k segment when the chain is in conformation α. Using $\langle x_0\rangle = \langle y_0\rangle = 0$ to denote the headgroup position, then for a fluid membrane $\langle x_k\rangle = \langle y_k\rangle = 0$ for all chain segments k. σ_{xy}^{k} is thus a measure of the lateral fluctuations of the kth segment around the membrane normal (originating from the headgroup). We note, as expected, that as k increases (i.e., towards the chain terminus), σ_{xy}^{k} also increases, indicating a higher degree of chain flexibility and lateral mobility. Furthermore, and again as expected, the amplitude of the fluctuations increase as the average cross-sectional area per chain, a, increases. All these findings are consistent with those inferred from the behavior of the profile of orientational bond order parameters.

The σ_{xy}^{k} have been measured for DPPC chains by incoherent quasi-elastic neutron scattering.[59] These measurements suggest, for a = 29.6 Å^2, that σ_{xy}^{k} varies nearly linearly from ~0.6 Å for k = 1 to σ_{xy} ~7 Å for k = 15. The calculated results shown in Figure 5 are in good agreement with these findings.

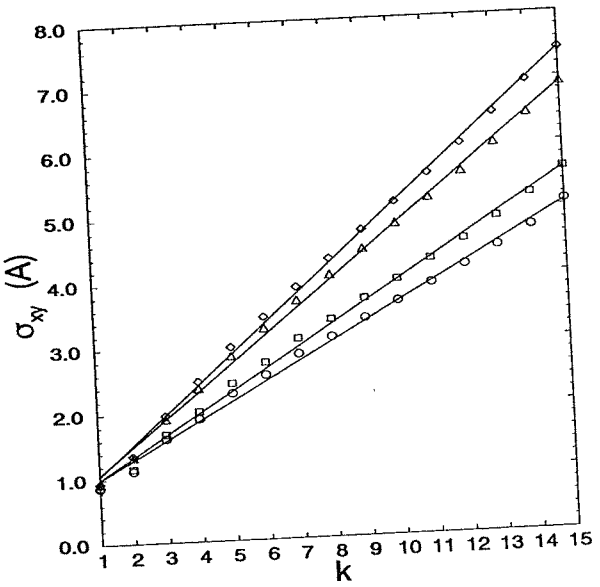

Figure 5 The lateral fluctuations (root mean square, in-plane, deviations) of the carbon atoms (k = 1,...,15) of DPPC calculated by the mean field theory (adapted from Reference 31). ○, □, Δ, and ◇ correspond to membranes in which the average cross sectional area per chain is a = 25.5, 26.6, 29.6, and 31.3 Å^2, respectively. The straight lines are linear fits. The calculated results show good agreement with experiments.[59] (From Fattal, D. R. and Ben-Shaul, A., *Biophys. J.*, 67, 983, 1994. With permission.)

We have shown in this section that the predictions of the mean field theory outlined in Section 2 show generally good agreement with observed experimental and computer simulation data. Good qualitative and often quantitative agreement has also been found with respect to other measurable properties, such as curvature elastic constants of mixed monolayers and bilayers.[6] Encouraged by these confirmations of the simple mean field theory we turn, in the following sections, to describe some of its applications to more complex phenomena.

IV. LIPID-PROTEIN INTERACTION

The presence of a hydrophobic "solute", such as the hydrophobic part of an integral protein, modifies the conformational properties of the lipids around it. In general, this "perturbation" increases the free energy of the surrounding lipids, so that when two or more hydrophobic solutes are in close proximity to each other the lipid-mediated interaction between them is attractive, thus favoring solute aggregation. The driving force for this aggregation is the tendency to minimize the contact area, and hence the extent of lipid perturbation, between the hydrophobic solutes and their surrounding lipid chains.

Various theoretical models have been proposed to describe and calculate the effects of an integral protein, usually treated as a rigid hydrophobic perturbation, on the lipid environment.[7,18,60-72] Some of those are continuum theories, based on treating the lipid bilayer as an elastic sheet of finite thickness. Several other statistical thermodynamic theories invoke Landau-type expansions of the free energy in terms of some order parameter, e.g., the "hydrophobic mismatch" (the difference between the protein and bilayer hydrophobic thickness[71]), addressing such issues as the effect of proteins on the solid/fluid ("gel-liquid crystal") transition temperature of the membrane. Very few models have considered the lipid-protein interaction on a molecular level. One such model, based on the molecular theory presented in Section II, will be outlined in this section.[7] Before turning to a more detailed description of this model it should be stressed that, as is often the case, the different theoretical approaches to the very complex issue of lipid-protein interaction should be regarded as complimentary rather than contradictive. For instance, the continuum elastic theories,[62-65] which are inherently valid for perturbations which are large on a molecular scale, are useful for understanding long-range elastic interactions between inclusions. Simple phenomenological approaches, such as the "mattress mode",[71] are useful for understanding the qualitative trends on membrane phase transitions as a function of the hydrophobic mismatch. Molecular

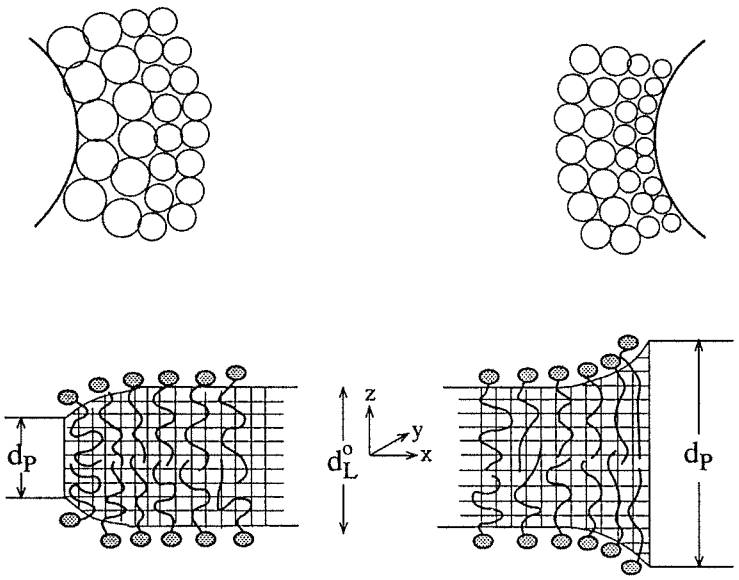

Figure 6 Schematics of the lipid-protein interaction model described in the text (adapted from Reference 7). Bottom panel is a "side view" of the bilayer, depicting the protein as a rigid wall of thickness d_P, either larger (right, "positive mismatch") or smaller (left, "negative mismatch") than the unperturbed bilayer thickness d_L^0. The chains in the vicinity of the protein are either stretched (when $d_P > d_L^0$) or compressed (when $d_P < d_L^0$) in order to bridge over the hydrophobic mismatch. The top panel is a "top view" of the membrane illustrating the corresponding changes in the average cross sectional area per chain as a function of the distance from the protein. (From Fattal, D. R. and Ben-Shaul, A., *Biophys. J.*, 65, 1795, 1993. With permission.)

models of the type presented below can provide numerical estimates on the lipid-protein interaction free energy, the range of perturbation of the lipid environment, and the origin of its dependence on the hydrophobic mismatch. Finally, it should be noted that all types of models mentioned above, including the one described below, expose only one aspect of the very complex and diverse phenomenon of lipid-protein interaction. More explicitly, by treating the protein as a rigid hydrophobic solute, we ignore not only the details of its complex structure but also the various electrostatic and steric interactions prevailing both in the core and in the interfacial regions.

Let d_L^0 denote the thickness of the lipid hydrophobic core. It is commonly assumed that when a rigid protein (or other inclusion) of hydrophobic thickness $d_P \sim d_L^0$ is incorporated into the membrane, the flexible lipid chains around it will adjust their length so as to shield the protein from direct contact with the surrounding water (see Figure 6). Using $d_L(x)$ to denote the bilayer thickness at a distance x from the protein, this assumption implies that $d_L(0) = d_P$. The variation of $d_L(x)$, between d_P at $x = 0$ are d_L^0 at $x \to \infty$, will be modeled as

$$d_L(x) = d_L^0 + \left(d_P - d_L^0\right)\exp\left(-x/\xi\right) \tag{25}$$

with ξ measuring the range (or the "coherence length") of the perturbation. The model treats ξ as a variational parameter whose value is determined by minimization of the total perturbation free energy. The exponential variation of the membrane thickness profile (Equation 25) has been derived by some of the Landau-type theories of lipid-protein interaction.[67,68] Yet in the present model it should only be regarded as a convenient parametrization of $d_L(x)$. In fact, some of the continuum elastic theories of lipid-protein interaction predict more complicated, including nonmonotonic, functional forms for $d_L(x)$.[63-65]

In the model illustrated in Figure 6 the protein is treated as a rigid cylinder embedded in the membrane. The diameter, D, of the cylinder cross section is assumed to be much larger than the average lateral dimension of the lipid chains, i.e., $D >> a^{1/2}$, where a is the average cross-sectional area per chain. Accordingly, to the lipids in its periphery the protein appears as a planar wall. Free energy calculations have been performed assuming that the protein wall is flat and is extending normally and symmetrically around the bilayer midplane.[7] Other geometries, e.g., a conical inclusion, can be treated similarly.

Assuming that the protein wall is parallel to the zy plane (z is the direction normal to the membrane plane), the lipid-protein interaction free energy per unit length of the protein perimeter (along the y direction) is given by

$$\Delta F = 2\int dx\left[\sigma(x)f(x) - \sigma^0 f^0\right] \tag{26}$$

where $f(x)$ is the local free energy per molecule at distance x from the protein and $\sigma(x)dxdy$ is the number of molecules originating from a small area element $dxdy$ of one of the two membrane interfaces. (More precisely, $dxdy$ is the projection of this area element onto the bilayer midplane.) σ^0 and f^0 are the corresponding quantities for the unperturbed membrane; that is, $\sigma^0 = \sigma(x)$ and $f^0 = f(x)$ as $x \to \infty$. The factor 2 in front of the integral accounts for the two leaflets of the bilayer.

In the planar bilayer $\sigma^0 = 1/a^0$, where $a^0 = 2v/d_L^0$ is the average area per chain; v denotes the volume of the hydrophobic tail. Assuming, as we did throughout this chapter, that the hydrophobic core is uniform and liquid-like, we have $\sigma(x) = 2v/d_L(x)$. Note, however, that except for the planar bilayer $\sigma(x) \neq 1/a(x)$, where $a(x)$ is the average local interface area per chain in the vicinity of the protein. This latter quantity is given by

$$a(x) = \frac{2v}{d_L(x)}\left\{1 + \frac{1}{4}\left(\frac{\partial d_L(x)}{\partial x}\right)^2\right\}^{1/2} \tag{27}$$

As in Section 2, the free energy per molecule can be expressed as a sun of tail, surface, and headgroup contributions:

$$f(x) = f_t(x) + f_s(x) + f_h(x) \tag{28}$$

The tail free energy and the corresponding spd are given By equations 13 and 14, respectively, with $\mathbf{s} \to x$ and $\mathbf{r} \to x,z$. The numerical calculation of $f_t(x)$ is considerably more complex than in the planar bilayer case, since $\lambda = \lambda(x,z)$ varies along both x and z, whereas for the planar bilayer $\lambda \to \pi(z)$ is only a function of z. Nevertheless, the calculations are feasible and representative numerical results will be shown below. In these calculations the surface free energy is modeled as $f_s = \gamma a(x)$, with $\gamma = 0.12$ KT/Å^2, and $f_h(x)$ is represented by the simple form $f_h(x) = C/a(x)$, with $a(x)$ given by Equation 27. The parameter C was chosen such that for a planar bilayer composed of $C_{14}(\mathcal{P}\text{–}(CH_2)_{13}\text{–}CH_3)$ lipids the equilibrium area per chain is $a_0 \cong 32$ Å^2 (see Figure 2).

The perturbation free energy ΔF of the C_{14} bilayer is shown in Figure 7 for three choices of the headgroup interaction parameter: $C = 48$ kT, 12 kT, and 0. First we note that $\Delta F \neq 0$ even for the case where no hydrophobic mismatch occurs, when $d_P = d_L^0$. In this case there is no contribution to ΔF from the surface ($\Delta F_s = 0$) or headgroup ($\Delta F_h = 0$) terms; only $\Delta F_t > 0$. Even though there is no change in the average chain length, the presence of the impenetrable protein wall reduces the conformational freedom of nearby chains, resulting in excess chain orientational ordering and non-negligible positive contribution to F_t. These notions are confirmed by explicit calculations of bond orientational order parameter profiles, showing increased $\langle S_k \rangle$ values for chains near the protein as compared to those away from it.[7] The chain conformational calculations also show a finite (though small) average tilt angle of the chains (away from the wall). It should be noted that the first molecular model of lipid-protein interaction, which was proposed by Marčelja, has been formulated for the $d_P = d_L^0$ case.[18] In Marčelja's model, like in the one presented here, $\Delta F_t > 0$ due to the loss of lipid chain conformational freedom in vicinity of the protein.[18]

When $d_P > d_L^0$ the lipid tails are stretched beyond their length in the unperturbed membrane, resulting in $\Delta F_t > 0$. In parallel, the average area per headgroup decreases[26] and consequently $\Delta F_s < 0$. The opposite behavior characterizes the case $d_P < d_L^0$. The contribution of headgroup repulsion (ΔF_h– to ΔF is, at least according to the model described, small compared to ΔF_s and ΔF_t. Thus, since as $d_P - d_L^0$ increases ΔF_t increases whereas ΔF_s decreases, the minimum of $\Delta F = \Delta F_t + \Delta F_s + \Delta F_h \simeq \Delta F_t + \Delta F_s$ is generally around $d_P - d_L^0 = 0$. However as seen in Figure 6, the minimum of ΔF shifts to a negative $d_P - d_L^0$ value when the strength of headgroup repulsion increases. In other words, negative hydrophobic mismatch can in fact relieve some of the lipid-protein interaction free energy when headgroup repulsion is strong. Similarly,

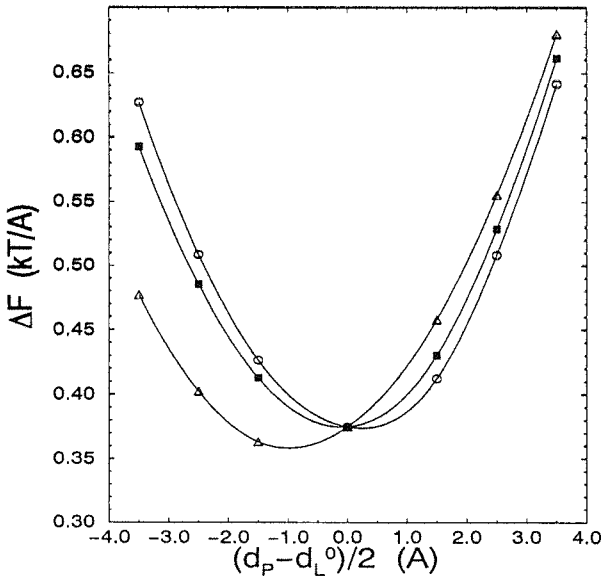

Figure 7 The lipid-protein interaction free energy (per unit length of perimeter length) for a bilayer of C_{14} chains, as a function of the hydrophobic mismatch (adapted from Reference 7). ○, ■, and Δ correspond to three different choices of the headgroup repulsion strength, $C = 0$, 12, 48 kT, respectively. (From Fattal, D. R. and Ben-Shaul, A., *Biophys. J.*, 65, 1795, 1993. With permission.)

positive mismatch can reduce ΔF (compared to the case $d_P = d_L^0$) in the case of strong chain repulsion. This effect has recently been predicted by Safran and Dan using a continuous elastic theory for the effect of hydrophobic inclusions on membrane properties.[64,65] Its origin, according to their analysis, is the nonzero spontaneous curvature of the monolayers comprising the bilayer. To understand the effect it is worthwhile to elaborate on the role of spontaneous curvature in lipid bilayers.

Consider one of the two monolayers comprising a lipid bilayer and assume it is planar. The three forces, headgroup repulsion, surface tension, and chain repulsion, balance each other at some equilibrium area per chain, a_{eq}. These forces also exert moments which may prefer a finite "spontaneous" curvature for the monolayer. The curvature may be either positive (the hydrocarbon-water interface convex towards the water), negative, or zero. Large moments of headgroup repulsion will tend to induce positive spontaneous curvature. Large moments of chain repulsion will act in the opposite manner. When two monolayers are brought into contact to form a planar bilayer, both are "frustrated" energetically since their curvature is not the optimal (spontaneous) one. Yet the planar bilayer geometry usually involves the least curvature energy cost for the two monolayers. Now suppose that headgroup repulsion is strong enough to favor positive spontaneous curvature for the monolayer. If $d_P < d_L^0$ then the lipids around the protein wall are packed with positive spontaneous curvature (see Figure 5), thus relieving some of the frustration energy associated with the formation of the planar bilayer. The case $C = 48$ kT in Figure 6 corresponds to strong headgroup repulsion and hence positive spontaneous curvature. Indeed, we note that for this case the minimum in ΔF takes place at a negative value of $d_P - d_L^0$. Similarly, stronger chain repulsion would shift the minimum towards positive $d_P - d_L^0$ values.

Various other structural and thermodynamic characteristics of the lipid-protein bilayer can be derived from the model described in this section. One result of particular interest is the spatial range of the perturbation, ξ. The perturbation of lipid order by the protein wall extends to ~ 3ξ. The calculations show that $\xi \sim 5$ Å. Since, typically, the lateral dimension of a lipid chain is $a^{1/2} \simeq 5$ to 6 Å, it follows that the range of perturbation corresponds to just a few molecular diameters.

V. THE VESICLE–MICELLE TRANSITION

Most lipid molecules in aqueous solution self-assemble spontaneously into extended 2D bilayers. The spontaneous (equilibrium, minimal free energy) curvature of bilayers is generally zero; i.e., they tend to

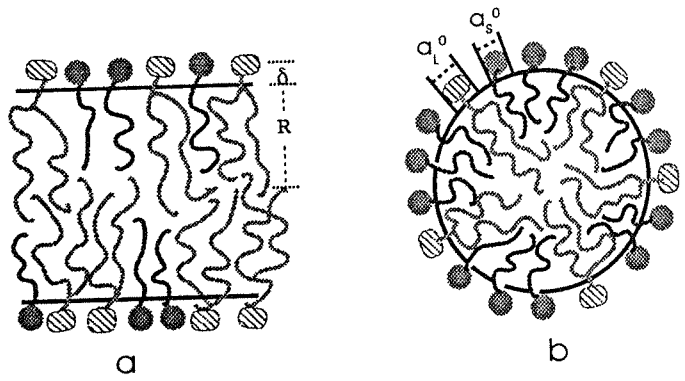

Figure 8 Schematic illustration of a mixed lipid surfactant bilayer (a) and a mixed micelle (b) (adapted from Reference 32). a_L^0 and a_S^0 are the bare headgroup areas of the two amphiphilic components, δ is the distance from the plane of headgroup repulsion to the hydrocarbon-water interface. (From Fattal, D. R., Andelman, D., and Ben-Shaul, A., *Langmuir,* submitted.)

be planar. To avoid the excess free energy associated with the exposure of their edges to water, the bilayers often close on themselves to from vesicles, at least in dilute solutions.[73] At higher lipid concentrations they may organize into multilamellar structures.[73,74] Other, nonlipid amphiphiles, which in dilute solution self-assemble into high-curvature aggregates such as cylindrical micelles, usually organize into multilamellar phases at higher concentration. These phases are stabilized by interaggregate interactions which overcome the intrinsic preference of the molecules to pack in highly curved aggregates.

Surfactant molecules, such as octylglucoside or bile salts, form micelles in dilute solution, reflecting their high spontaneous curvature.[75,76] Recall that any point of a curved surface can be characterized by two local principal curvatures, c_1 and c_2, with $R_i = 1/c_i$ $(i = 1,2)$ denoting the corresponding radius of curvature. Thus, for example, the hydrocarbon-water interface of a spherical micelle of radius R is characterized everywhere by $c_1 = c_2 = 1/R$, with $R \leq l$, where l is the length of the fully extended amphiphile tail. Similarly, in cylindrical micelles (except at the hemispherical caps), $c_1 = 1/R_1$ whereas $c_2 = 0$, R_1 denoting the radius of the cylinder cross section ($R_1 \leq l$) and $R_2 \to \infty$ denoting the radius of the cylinder axis. In planar bilayers $c_1 = c_2 = 0$, and in spherical vesicles of radius R, $c_1 = c_2 = 1/R$, with $R >> l$.

Consider now a dilute binary aqueous solution of lipids whose spontaneous aggregation geometry is planar ($c_1 = c_2 \simeq 0$) and surfactants which in dilute solution prefer organization in, say, cylindrical micelles ($c_1 \cong 1/l$, $c_2 = 0$). Let $\chi = \chi_L = N_L/(N_L + N_S) = N_L/N$ denote the mole fraction of lipids and $\chi_S = 1 - \chi$ the mole fraction of surfactants in solution, N_L and N_S denoting the number (or concentration) of lipid and surfactant molecules, respectively. (The mole fractions involve only the amphiphilic components, not the solvent; $\chi_S + \chi_L = 1$.) In the limits $\chi = 1$ and $\chi = 0$ the amphiphiles form lipid vesicles ($c_1 = c_2 \simeq 0$) and surfactant micelles, respectively. When a small amount of surfactant molecules is added to a system composed of lipid vesicles, a certain fraction of them (typically very small, corresponding to the cmc [critical micellar concentration][1,3-5]) are dispersed as monomers in the solution; the rest are incorporated ("solubilized") into the vesicles. As in ordinary binary mixtures, the thermodynamic driving force for the incorporation of the surfactant into the lipid bilayer is the mixing entropy, which overcounts the tendency of the surfactant and lipid molecules to pack, separately, according to their energetically preferred aggregation geometries. Similarly, upon adding small amounts of lipids to a surfactant-rich system they will be solubilized in the surfactant micelles (hardly any of them will be present as monomers, due to the extremely low cmc of lipids). Schematic illustrations of a mixed lipid-surfactant bilayer and a mixed cylindrical micelle are shown in Figure 8.

In ordinary binary molecular solutions, say of A and B molecules, phase separation of an A-rich and a B-rich phase can take place, provided the effective A-B interaction $w = w_{AB} - (w_{AA} + w_{BB})/2$ is repulsive, i.e., $w > 0$; $w_{IJ}(I = A,B)$ denotes the interaction energy between I and J molecules (integrated over distances and orientations or, in lattice models, between neighboring molecules). More precisely, phase separation occurs below a certain critical temperature T_c (proportional to w) and only over a certain range of (intermediate) compositions, which broadens as T decreases farther from T_c.

An analogous scenario can, and usually does, happen in aqueous solutions of lipids and surfactants. The analogue of w in these systems is the difference in the packing (free) energy of surfactants and lipids in a mixed system, compared to their packing in separate aggregates. The coexisting phases in lipid-surfactant solutions, if and when phase separation takes place, are vesicles with amphiphile composition x_v (v = vesicle) and micelles with composition x_m (m = micelle), such that $x_m < x_v$. The separated phases appear in different regions of space (vesicles and micelles floating in the aqueous solution) and are characterized by very different symmetries: nearly planar lipid-rich bilayer vesicles vs. elongated (or sometimes globular) surfactant-rich micelles.

This qualitative thermodynamic scenario does indeed take place in many lipid-surfactant systems[77-81] and is of considerable biological importance, e.g., for membrane reconstitution.[76] What typically happens is that a lipid vesicle can take up surfactant molecules up to a limit corresponding to a lipid content x_v. Beyond that limit the vesicles break into micelles with lipid content x_m. In lecithin-bile salt and lecithin-octylglucoside mixtures the compositions of coexisting vesicles and micelles are $x_v \sim 1/2$ and $x_m \sim 1/4$.

A simple qualitative theoretical model of the vesicle–micelle transition has recently been formulated by Andelman, Kozlov, and Helfrich.[83] These authors have expressed the free energy of both the (mixed) bilayer and micelle as a sum of a curvature energy term and a mixing entropy term. Explicitly, the average (Helmholtz) free energy per molecule in each of the two aggregation geometries is written as

$$\psi(x) = \frac{1}{2}\kappa\left[c_1 + c_2 - c_0(x)\right]^2 + kT\left[x\ln x + (1-x)\ln(1-x)\right] \tag{29}$$

with x denoting the lipid mole fraction in the aggregate. (Actually in Reference 83 x denotes the area fraction of lipids, measured at the hydrocarbon-water interface. This difference is irrelevant for the present discussion and for understanding this phenomenon.) The second term in Equation 29 is an ideal mixing entropy contribution. The first term is the common, Helfrich form of the bending free energy of a membrane.[38] κ denotes the curvature (splay) elastic modulus and $c_0(x)$ is the spontaneous curvature of an aggregate with composition x. The spontaneous curvature has been assumed to vary linearly with x, say from $c_0(x = 0) = 1/R$, corresponding to a cylindrical surfactant micelle of radius R, to $c_0(x = 1) = 0$, corresponding to a planar lipid bilayer (or a very large vesicle). κ was treated as a constant, independent of x or aggregation geometry. Then $f(x)$ is calculated for the vesicle ($c_1 = c_2 \simeq 0$) and for the cylindrical micelle ($c_1 = 1/R, c_2 = 0$), and by equating the chemical potentials of the lipid and surfactant in the two geometries (common tangent construction) a general expression can be derived for the lipid composition of the vesicle and micelle at the transition.

This simple and elegant model can predict some interesting qualitative trends, e.g., the dependence of the coexisting compositions on $c_0(x)$, T and κ. Yet it must be remembered that the bending energy term in Equation 29 is valid only for small deviations, mainly of planar films, around the equilibrium curvature. Vesicles and cylindrical micelles correspond to very different equilibrium curvatures. It is highly unlikely that the harmonic (quadratic) form of the bending energy, with the same κ for all geometries, can faithfully describe the geometry dependence of the amphiphile packing free energy. Molecular-level calculations of the type described in previous sections confirm this question. Furthermore, molecular calculations of κ show that it depends sensitively on x.[6,84] (For instance, the bending rigidity of lipid membranes decreases rapidly upon adding short-chain surfactants to the bilayer.) Interestingly enough, recent calculations of this kind show that in some mixtures $c_0(x)$ varies nearly linearly with x over a wide range of composition.[84]

An obvious alternative to the first term in Equation 29 is to calculate the packing free energy of mixed lipid-surfactant bilayers and micelles using the molecular mean field theory described in Sections 2 to 4. Thus, instead of Equation 29 one writes

$$\psi_g(x) = x f_g^L(x) + (1-x) f_g^S(x) + kT\left[x\ln x + (1-x)\ln(1-x)\right] \tag{30}$$

with $f_g^L(x)$ denoting the packing free energy per lipid molecule in a mixed aggregate of geometry g (g = vesicle, micelle) and composition x. Then, plotting $\psi_g(x)$ vs. x for the two aggregation geometries one can evaluate the coexisting compositions, x_v and x_m, using common tangent construction.

The results of one calculation of this kind, corresponding to a given set of molecular parameters (see below), are shown in Figure 9. Also marked on the figure is the composition $x_v = 0.47$, below which the

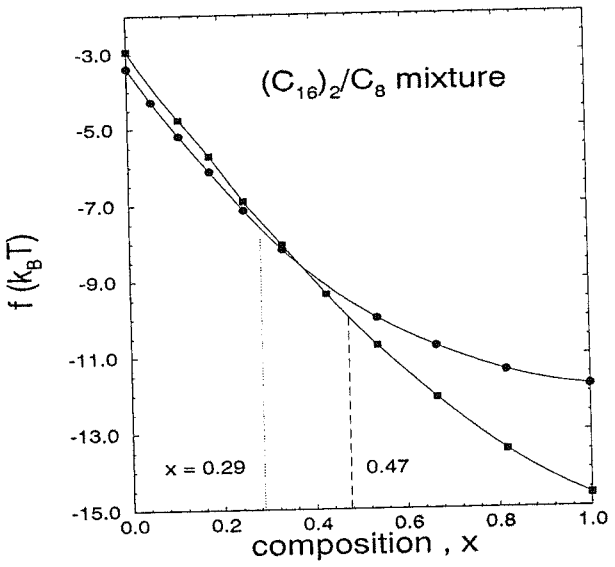

Figure 9 The average free energy per molecule in a mixed $(C_{16})_2/C_8$ lipid surfactant bilayer (■) and cylindrical micelle (●) as a function of lipid mole fraction (adapted from Reference 32). The compositions of the bilayer (x = 0.47) and micelle (x = 0.29) at the vesicle-micelle transitions are evaluated by common tangent construction (corresponding to equating the chemical potentials of each component in both aggregation geometries). (From Fattal, D. R., Andelman, D., and Ben-Shaul, A., *Langmuir*, submitted.)

vesicle is unstable, and the composition $x_m = 0.29$, corresponding to the micelles initially formed when the vesicles break. Conversely, x_m is the maximal lipid content in a cylindrical micelle, beyond which vesicles of composition x_v begin to form.

The results shown in Figure 9 as well as several additional cases are discussed in more detail elsewhere.[32] Here we shall only mention the basic assumptions. The system considered is a mixture of saturated double-chain lipids $\mathcal{P}_L$–$[(CH_2)_{15}$–$CH_3]_2$ and short single-chain surfactants $\mathcal{P}_S$–$(CH_2)_7$–CH_3, with $\mathcal{P}_L$ and $\mathcal{P}_S$ denoting the lipid and surfactant headgroups, respectively. As in previous sections, the free energy of the mixed bilayer, and the mixed cylinder, has been expressed as a sum of tail (f_t), surface ($f_s = \gamma a$), and headgroup contributions. The headgroup contribution to $xf_g^L(x) + (1 - x)f_g^S(x)$ has been modeled as a steric repulsion free energy:[44]

$$f_h^g = -kT\ln\left(1 - a_h / \bar{a}^g\right) \tag{31}$$

Here $\bar{a}^g = \bar{a}^g(x)$ is the average area per headgroup in aggregates of geometry $g(g = v,m)$. This area is measured at the plane of headgroup repulsion, assumed to be located at distance δ from the hydrocarbon-water interface. For a planar bilayer (large vesicle) $\bar{a}^v = a^v$, where a^v is the area per headgroup at the interface; for a cylinder micelle of radius R, $\bar{a}^m = a^m\,(1 + \delta/R)$. The quantity $a_h = a_h(x) = xa_h^L + (1 - x)a_h^S$ is the average bare (hard-core) headgroup area per molecule, at the plane of headgroup interactions. a_h^L and a_h^S denote, respectively, the bare headgroup areas per lipid and per surfactant molecule.

The surface contribution to the free energy is modeled as

$$f_s^g(x) = x\gamma\left(a^g - a_L^h\right) + (1-x)\gamma\left(a^g - a_s^h\right) = \gamma\left(a^g a_h\right) \tag{32}$$

The chain conformational contributions were calculated using the mean field theory for mixed systems, as outlined in Section 2.

The numerical values used for the specific calculation shown in Figure 9 were $\gamma = 0.12$ kT/Å, $a_h^L = 42$ Å^2, $a_h^S = 50$ Å^2, and $\delta = 1.1$ Å. The choice of a_h^L ensures that the equilibrium average cross-sectional area per molecule in a pure lipid bilayer is 68 Å^2, as commonly found for lecithin bilayers.[80] The numerical values of a_h^S and δ (which in Reference 78 were treated as parameters controlling the spontaneous

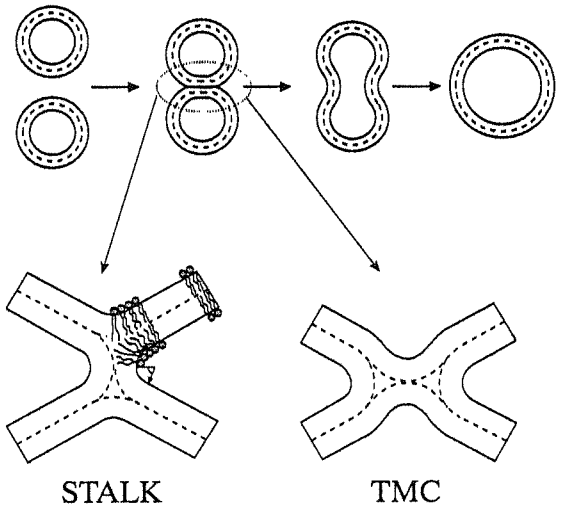

Figure 10 Schematic illustration of the several stages in the fusion of vesicle bilayers (top). The bottom figure shows in more detail two of the proposed structural intermediates along the fusion pathway.[85,86]

curvature of the surfactant) ensure that the optimal packing geometry of the C_8 surfactant molecules in dilute solution is a cylindrical micelle, with an average area per surfactant headgroup $a \simeq 55$ Å^2.

The free energy per molecule has been calculated as a function of composition x for both geometries, and the values of the amphiphile in the vesicles and the micelles at the transition ($x^v = 0.47$ and $x^m = 0.29$) were determined by common tangent construction. These values for x^v and v^m are in the range observed experimentally.[79-82] The molecular parameters used (a_h^L,a_h^S,γ,δ) are all very reasonable and, moreover, have been adjusted so as to ensure micelle formation at $x \to 0$ and vesicle formation at $x \to 1$. Nevertheless, it must be mentioned that the uncertainties involved in choosing these parameters are considerable. Different choices of, say, a_h^L and δ can lead to substantial shifts in the values inferred for x_v and x_m. The semiempirical adjustment of such parameters by referring to limiting (i.e., the pure) cases seems, at present, to be the most plausible procedure. Notwithstanding these reservations, the model described in this section does account for the basic interactions and trends characteristic of the vesicle–micelle transition. Other structural transitions, such as from lamellar to inverted hexagonal or cubic phases, can possibly be accounted for using a similar approach.

VI. SUMMARY

In some cases, especially in systems of low symmetry such as the lipid-protein membrane, the molecular mean field theory described in this chapter requires some nontrivial calculations. Nevertheless, the computational effort involved is still substantially less than that required in large-scale computer simulations. Various other systems and processes in membrane biophysics can be studied and analyzed on a molecular level using this approach. These include, for example, the thermodynamic stability of mixed vesicles, pore (and other defect) formation in membranes, and the phase transition from lamellar to inverted hexagonal phases. Let us conclude this section by mentioning some very preliminary results concerning an issue of considerable biological relevance: the fusion of lipid vesicles.

Several authors have proposed phenomenological models for the mechanism and the structural intermediates involved in the process of membrane fusion[85-87] after the initial adhesion process.[88,90] One of the suggested pathways, the "modified Stalk mechanism" suggested by Siegel,[45] is schematically illustrated in Figure 10. Siegel has also estimated the excess free energies associated with the formation of the structural intermediates, using the continuum theory for membrane curvature and stretching elasticity.[38]

We have recently performed calculations of the kind described in Sections 2 and 3 for the excess free energy of the "Stalk" intermediate (Figure 10) for a pure lipid membrane composed of C_{14} chains. The results obtained are $\Delta F \geq 100$ kT. These numbers are in surprisingly good agreement with those obtained using the continuum theory. The agreement is surprising because the structural intermediates involve

variations of packing geometry extending over only a few molecular diameters. However, additional calculations are called for before this good agreement can be confirmed.

ACKNOWLEDGMENT

We would like to thank E. Sackmann, W. M. Gelbart, I. Szleifer, D. Lichtenberg, Y. Barenholz, D. Andelman, Y. Talmon, S. Safaran, M. Kozlov, and D. Siegel for helpful discussions and comments on the topics outlined in this chapter. The financial support of the National Science Foundation administered by the Israel Academy of Science and Humanities and the Yeshaya Horowitz Association is gratefully acknowledged. The Fritz Haber Research Center, where this research was done, is supported by the Minerva Gesellschaft für die Forschung, mbH, Munich, Germany.

REFERENCES

1. **Ben-Shaul, A. and Gelbart, W. M.,** Statistical thermodynamics of amphiphile self-assembly: structure and phase transitions in micellar solutions, in: *Micelles, Membranes, Microemulsions and Monolayers,* Gelbart, W. M., Ben-Shaul, A., and Roux, D., Eds., Springer-Verlag, New York, 1994, chap. 1.
2. **Ben-Shaul, A.,** Molecular theory of chain packing, elasticity and lipid protein interaction in lipid bilayers, in: *Handbook of Physics of Biological Systems,* Vol. 1, Lipowsky, R. and Sackmann, E., Eds., Elsevier Science, Amsterdam, 1995, chap. 7.
3. **Tanford, C.,** *The Hydrophobic Effect,* 2nd ed., Wiley-Interscience, New York, 1980.
4. **Israelachvili, J. N.,** *Intermolecular and Surface Forces,* Academic Press, London, 1985.
5. **Wennerström, H. and Lindman, B.,** Micelles, physical chemistry of surfactant association, *Phys. Rep.,* 52, 1, 1979.
6. **Szleifer, I., Kramer, D., Ben-Shaul, A., Gelbart, W. M., and Safran, S. A.,** Molecular theory of curvature elasticity in surfactant films, *J. Chem. Phys.,* 92, 6800, 1990.
7. **Fattal, D. R. and Ben-Shaul, A.,** A molecular model for lipid-protein interaction in membranes: the role of hydrophobic mismatch, *Biophys. J.,* 65, 1795, 1993.
8. **Carignano, M. A. and Szleifer, I.,** Statistical theory of grafted polymer layers, *J. Chem. Phys.,* 98, 5006, 1993.
9. **Heller, H., Schaefer, M., and Schulten, K.,** Molecular dynamics simulation of a bilayer of 200 lipids in the gel and in the liquid crystal phases, *J. Phys. Chem.,* 97, 8343, 1993.
10. **van der Ploeg, P. and Berendsen, H. J. C.,** Molecular dynamics of a bilayer membrane, *Mol. Phys.,* 49, 233, 1983; Egberts, E. and Berendsen, H. J. C., Molecular dynamics simulation of a smectic liquid crystal with atomic detail, *J. Phys. Chem.,* 89, 3718, 1988.
11. **Biswas, A. and Schurman, B. L.,** Molecular dynamics simulation of a dense model bilayer of chain molecules with fixed head groups, *J. Chem. Phys.,* 95, 5377, 1991.
12. **Marrink, S. J., Berkowitz, M., and Berendsen, H. J. C.,** Molecular dynamics of a membrane/water interface: the ordering of water and its relation to the hydration force, *Langmuir,* 9, 3122, 1993.
13. **Raghavan, K., Reddy, M. R., and Berkowitz, M. L.,** A molecular dynamics study of the structure and dynamics of water between dilauroylphosphatidylethanolamine bilayers, *Langmuir,* 8, 233, 1992.
14. **Levine, Y. K., Kolinski, A., and Skolnick, J.,** Lattice dynamics study of a Langmuir monolayer of monounsaturated fatty acids, *J. Chem. Phys.,* 98, 7581, 1993; Levine, Y. K., Monte Carlo dynamics study of cis and trans unsaturated hydrocarbon chains, *Mol. Phys.,* 78, 619, 1993.
15. **Scott, H. L. and Cherng, S. L.,** Monte Carlo studies of phospholipid lamellae. Effects of proteins, cholesterol, bilayer curvature, and lateral mobility on order parameters, *Biochim. Biophys. Acta,* 510, 209, 1978.
16. **Ipsen, J. H., Jørgensen, K., and Mouritsen, O. G.,** Density fluctuations in saturated phospholipid bilayers increase as the acyl-chain length decreases, *Biophys. J.,* 58, 1099, 1990.
17. **Marelja, S.,** Chain ordering in liquid crystals. II. Structure of bilayer membranes, *Biochim. Biophys. Acta,* 367, 165, 1974.
18. **Marelja, S.,** Lipid-mediated protein interaction in membranes, *Biochim. Biophys. Acta,* 455, 1, 1976.
19. **See e.g., de Gennes, P. G. and Prost, J.,** *The Physics of Liquid Crystals,* 2nd ed., Clarendon Press, Oxford, 1993.
20. **Dill, K. A. and Flory, P.,** Interphases of chain molecules: monolayers and lipid bilayer membranes, *Proc. Natl. Acad. Sci. U.S.A.,* 77, 3115, 1980.
21. **Dill, K. A. and Stigter, D.,** Lateral interactions among phosphatidylcholine and phosphatidylethanolamine head groups in phospholipid monolayers and bilayers, *Biochem. J.,* 27, 3446, 1988.
22. **Gruen, D. W. R.,** A model for the chains in amphiphilic aggregates. I. Comparison with a molecular dynamics simulation of a bilayer, *J. Phys. Chem.,* 89, 146, 1985.
23. **Gruen, D. W. R.,** The standard picture of ionic micelles, *Prog. Colloid Polymer Sci.,* 70, 6, 1985.
24. **Ben-Shaul, A., Szleifer, I., and Gelbart, W. M.,** Statistical thermodynamics of amphiphile chains in micelles, *Proc. Natl. Acad. Sci. U.S.A.,* 81, 4601, 1984.
25. **Ben-Shaul, A., Szleifer, I., and Gelbart, W. M.,** Chain organization and thermodynamics in micelles and bilayers. I. Theory, *J. Chem. Phys.,* 83, 3597, 1985.

26. **Szleifer, I., Ben-Shaul, A., and Gelbart, W. M.,** Chain organization and thermodynamics in micelles and bilayers. II. Model calculations, *J. Chem. Phys.*, 83, 3612, 1985.
27. **Szleifer, I., Ben-Shaul, A., and Gelbart, W. M.,** Statistical thermodynamics of molecular organization in mixed micelles and bilayers, *J. Chem. Phys.*, 86, 7094, 1987.
28. **Szleifer, I., Ben-Shaul, A., and Gelbart, W. M.,** Chain statistics in micelles: effects of surface roughness and internal energy, *J. Chem. Phys.*, 85, 5345, 1986.
29. **Szleifer, I., Ben-Shaul, A., and Gelbart, W. M.,** Chain packing statistics and thermodynamics of amphiphilic monolayers, *J. Phys. Chem.*, 94, 5081, 1990.
30. **Ben-Shaul, A. and Gelbart, W. M.,** Alkyl chain packing in micelles and bilayers, *Annu. Rev. Phys. Chem.*, 36, 179, 1985.
31. **Fattal, D. R. and Ben-Shaul, A.,** Mean-field calculations of chain packing and conformational statistics in lipid bilayers: comparison with experiments and molecular dynamics studies, *Biophys. J.*, 67, 983, 1994.
32. **Fattal, D. R., Andelman, D., and Ben-Shaul, A.,** The vesicle-micelle transition in mixed lipid-surfactant systems: a molecular model, *Langmuir*, 11, 1154, 1995.
33. **Scheutjens, J. M. H. M. and Fleer, G. J.,** Statistical theory of the adsorption of interacting chain molecules. I. Partition function, segment density distribution, and adsorption isotherms, *J. Phys. Chem.*, 83, 1619, 1979.
34. **Leermakers, F. A. M. and Scheutjens, J. M. H. M.,** Statistical thermodynamics of association colloids. I. Lipid bilayer membranes, *J. Chem. Phys.*, 89, 3264, 1988.
35. **Barneveld, P. A., Hesselink, D. E., Leermakers, F. A. M., Lyklema, J., and Scheutjens, J. M. H. M.,** Bending moduli and spontaneous curvature. II. Bilayers and monolayers of pure and mixed ionic surfactants, *Langmuir*, 10, 1084, 1994.
36. **Meijer, L. A., Leermakers, F. A. M., and Nelson, A.,** Modelling of the electrolyte ion-phospholipid layer interaction, *Langmuir*, 10, 1199, 1994.
37. **Flory, P. J.,** *Statistical Mechanics of Chain Molecules*, Wiley-Interscience, New York, 1969.
38. **Helfrich, W.,** Elastic properties of lipid bilayers: theory and possible experiments, *Z. Naturforsch.*, 28c, 693, 1973; Helfrich, W., Blocked lipid exchange in lipid bilayers and its possible influence on the shape of vesicles, *Z. Naturforsch.*, 29c, 510, 1974.
39. **Evans, E. A. and Skalak, R.,** Mechanics and thermodynamics of biomembranes, in: *Critical Reviews in Bioengineering*, CRC Press, Boca Raton, FL, 1979, p. 181.
40. **Petrov, A. G. and Bivas, I.,** Elastic and flexoelectric aspects of out-of-plane fluctuations in biological and model membranes, *Prog. Surf. Sci.*, 16, 389, 1984.
41. **Lasic, D. D.,** The mechanism of vesicle formation, *Biochem. J.*, 256, 1, 1988.
42. **Stigter, D., Mingins, J., and Dill, K. A.,** Phospholipid interactions in model membrane systems. II. Theory, *Biophys. J.*, 61, 1616, 1992.
43. **Andelman, D.,** Electrostatic properties of membranes, in: *Handbook of Physics of Biological Systems*, Vol. 1, Lipowsky, R. and Sackmann, E., Eds., Elsevier Science, Amsterdam, 1995.
44. **Puvvada, S. and Blankschtein, D.,** Theoretical and experimental investigations of micellar properties of aqueous solutions containing binary mixtures of nonionic surfactants, *J. Phys. Chem.*, 96, 5579, 1992; Nagarajan, R., Molecular theory for mixed micelles, *Langmuir*, 1, 331, 1985.
45. **Cevc, G.,** Membrane electrostatics, *Biochim. Biophys. Acta*, 1031, 311, 1990.
46. **Ennis, J.,** Spontaneous curvature of surfactant films, *J. Phys. Chem.*, 97, 663, 1992.
47. **Winterhalter, M. and Helfrich, W.,** Bending elasticity of electrically charged bilayers: coupled monolayers, neutral surfaces, and balancing stresses, *J. Chem. Phys.*, 96, 327, 1992.
48. **Mitchell, D. J. and Ninham, B. W.,** Curvature elasticity of charged membranes, *Langmuir*, 5, 1121, 1989.
49. **Lekkerkerker, H. N. W.,** Contribution of the electric double layer to the curvature elasticity of charged amphiphilic monolayers, *Physica*, A159, 319, 1989.
50. **Lewis, B. A. and Engelman, D. M.,** Lipid bilayer thickness varies linearly with acyl chain length in fluid phosphatidylcholine vesicles, *J. Mol. Biol.*, 166, 211, 1983.
51. **Seelig, J. and Waespe-Šarčević, N.,** Molecular order in cis and trans unsaturated phospholipid bilayers, *Biochem. J.*, 17, 3310, 1978.
52. **Seelig, J. and Seelig, A.,** Lipid conformation in model membranes and biological membranes, *Q. Rev. Biophys.*, 13, 19, 1980.
53. **Bloom, M., Evans, E., and Mouritsen, O. G.,** Physical properties of the fluid lipid-bilayer component of cell membranes: a perspective, *Q. Rev. Biophys.*, 24, 293, 1991.
54. **Nagle, J. F.,** Area/lipid of bilayers from NMR, *Biophys. J.*, 64, 1476, 1993.
55. **Edholm, O.,** Order parameters in hydrocarbon chains, *Chem. Phys.*, 64, 259, 1982.
56. **Wiener, M. C. and White, S. H.,** Structure of a fluid dioleoylphosphatidylcholine bilayer determined by joint refinement of X-ray and neutron diffraction data. II. Distribution and packing of terminal methyl groups, *Biophys. J.*, 61, 428, 1992.
57. **Wiener, M. C. and White, S. H.,** Structure of a fluid dioleoylphosphatidylcholine bilayer determined by joint refinement of X-ray and neutron diffraction data. III. Complete structure, *Biophys. J.*, 61, 434, 1992.
58. **Small, D. M.,** *The Physical Chemistry of Lipids*, Plenum Press, New York, 1986.

59. **König, S., Pfeiffer, W., Bayerl, T., Richter, D., and Sackmann, E.,** Molecular dynamics of lipid bilayers studied by incoherent quasi-elastic neutron scattering, *J. Phys. II (Paris),* 2, 1589, 1992.
60. **Abney, J. R. and Owicki, J. C.,** Theories of protein-lipid and protein-protein interactions in membranes, in: *Progress in Protein-Lipid Interactions,* Watts, A. and de Pont, J. J. H. M., Eds., Elsevier, Amsterdam, 1985, 1.
61. **Mouritsen, O. G. and Bloom, M.,** Models of lipid-protein interactions in membranes, *Annu. Rev. Biophys. Biomol. Struct.,* 22, 145, 1993.
62. **Huang, H. W.,** Deformation free energy of bilayer membrane and its effect on gramicidin channel lifetime, *Biophys. J.,* 50, 1061, 1986.
63. **Helfrich, P. and Jakobsson, E.,** Calculation of deformation energies and conformations in lipid membranes containing gramicidin channels, *Biophys. J.,* 57, 1075, 1990.
64. **Dan, N., Pincus, P., and Safran, S. A.,** Membrane-induced interactions between inclusions, *Langmuir,* 9, 2768, 1993.
65. **Dan, N. and Safran, S. A.,** *J. Israel Chem. Soc.,* submitted, 1995.
66. **Caillé, A., Pink, D., De Verteuil, F., and Zuckermann, M. J.,** Theoretical models for quasi-dimensional mesomorphic monolayers and membrane bilayers, *Can. J. Phys.,* 58, 581, 1980.
67. **Owicki, J. C. and McConnel, H. M.,** Theory of protein-lipid and protein-protein interactions in bilayer membranes, *Proc. Natl. Acad. Sci. U.S.A.,* 76, 4750, 1979.
68. **Jähnig, F.,** Critical effects from lipid-protein interaction in membranes, *Biophys. J.,* 36, 329, 1981.
69. **Jähnig, F., Vogel, H., and Best, L.,** Unifying description of the effect of membrane proteins on lipid order. Verification for the melittin/dimyristoylphosphatidylcholine system, *Biochemistry,* 21, 6790, 1982.
70. **Scott, H. L. and Coe, T. J.,** A theoretical study of lipid-protein interactions in bilayers, *Biophys. J.,* 42, 219, 1983.
71. **Mouritsen, O. G. and Bloom, M.,** Mattress model of lipid-protein interactions in membranes, *Biophys. J.,* 46, 141, 1984.
72. **Sperotto, M. M. and Mouritsen, O. G.,** Dependence of lipid membrane phase transition temperature on the mismatch of protein and lipid hydrophobic thickness, *Eur. Biophys. J.,* 16, 1, 1988.
73. **Lasic, D. D.,** *Liposomes: From Physics to Applications,* Elsevier Science, Amsterdam, 1993.
74. **Gelbart, W. M., Ben-Shaul, A., and Roux, D.,** Eds., *Micelles, Membranes, Microemulsions and Monolayers,* Springer-Verlag, New York, 1994.
75. **Rosevear, P., VanAken, T., Baxter, J., and Ferguson-Miller, S.,** Alkyl glycoside detergents: a simpler synthesis and their effects on kinetic and physical properties of cytochrome c oxidease, *Biochemistry,* 19, 4108, 1980; VanAken, T., Foxall-VanAken, S., Casetleman, S., and Ferguson-Miller, S., Alkyl glycoside detergents: synthesis and applications to the study of membrane proteins, *Methods Enzymol.,* 125, 27, 1986.
76. **Jennis, R. B.,** *Biomembranes: Molecular Structure and Function,* Springer-Verlag, New York, 1989.
77. **Vinson, P. K., Talmon, Y., and Walter, W.,** Vesicle-micelle transition of phosphatidylcholine and octyl glucoside elucidated by cryo-transmission electron microscopy, *Biophys. J.,* 56, 669, 1989.
78. **Shurtenberger, P., Mazer, N., and Känzig, W.,** Micelle to vesicle transition in aqueous solutions of bile salt and lecithin, *J. Phys. Chem.,* 89, 1042, 1985.
79. **Almog, S., Litman, B. J., Wimley, W., Cohen, J., Wachtel, E., Barenholtz, E. J., Ben-Shaul, A., and Lichtenberg, D.,** State of aggregation and phase transformations in mixtures of phosphatidylcholine and octylglucoside, *Biochemistry,* 29, 4582, 1990.
80. **Ollivon, M., Eidelman, O., Blumenthal, R., and Walter, A.,** Micelle-vesicle transition of egg phosphatidylcholine and octyl glucoside, *Biochemistry,* 27, 1695, 1988; See also; Eidelman, O., Blumenthal, R., and Walter, A., Composition of octyl glucoside-phosphatidylcholine mixed micelles, *Biochemistry,* 27, 2839, 1988.
81. **Edwards, K., Gustafsson, J., Almgren, M., and Karlsson, G.,** Solubilization of lecithin vesicles by a cationic surfactant: intermediate structures in the vesicle-micelle transition observed by cryo-transmission electron microscopy, *J. Colloid. Interface Sci.,* 161, 299, 1993.
82. **Paternostre, M. T., Roux, M., and Rigaud, J. L.,** Mechanisms of membrane protein insertion into liposomes during reconstitution procedures involving the use of detergents. I. Solubilization of large unilamellar liposomes (prepared by reverse-phase evaporation) by Triton X-100, octyl glucoside, and sodium cholate, *Biochemistry,* 27, 2668, 1988.
83. **Andelman, D., Kozlov, M. M., and Helfrich, W.,** Phase transitions between vesicles and micelles driven by competing curvatures, *Europhys. Lett.,* 25, 231, 1994.
84. **May, S. and Ben-Shaul, A.,** Spontaneous curvature of mixed lipid vesicles, in preparation.
85. **Siegel, D. P.,** Energetics of intermediates in membrane fusion: comparison of stalk and inverted micellar intermediate mechanisms, *Biophys. J.,* 65, 2124, 1993.
86. **Kozlov, M. M., Leikin, S. L., Chernomordik, V., Markin, V. S., and Chizmadzhev, Y. A.,** Stalk mechanism of vesicle fusion. Intermixing of aqueous contents, *Eur. Biophys. J.,* 17, 121, 1989.
87. **Verkleij, A. J., VanEchteld, C. J. A., Gerritsen, W. J., Cullis, P. R., and DeKruijff, B.,** The lipidic particle as an intermediate structure in membrane fusion processes and bilayer to hexagonal H_{II} transitions, *Biochim. Biophys. Acta,* 600, 620, 1980.
88. **Leckband, D. E., Helm, C. A., and Israelachvili, J.,** Role of calcium in the adhesion and fusion of bilayers, *Biochemistry,* 32, 1127, 1993.
89. **Rand, R. P. and Parsegian, V. A.,** Hydration forces between phospholipid bilayers, *Biochim. Biophys. Acta,* 988, 351, 1989.